Real Time Kinematic GPS in an Urban Canyon Environment

Adeniyi Iyiade

University of Plymouth,
SEOES. Portland Square
PL4 8AA. Plymouth. UK
aiyiade@plymouth.ac.uk

Abstract

As Global Positioning Systems (GPS) measurements like other survey measurements are not devoid of errors. In Real Time Kinematic (RTK) positioning in an urban canyon environments where the GPS signals are blocked by high buildings and there are not enough satellites signals in estimating the positions of the user, computation of the antenna positioning is a major problem.

The research work uses an Extended Kalman Filter (EKF) as an attempt to reduce the effects of errors such as the atmospheric errors, multipath and receiver noise on GPS signals during transmission. However, some unmodelled biases still remain in the GPS observations, stochastic models were used as a quality indicator to identify and isolate such biases. The end result shows an improved coordinates solution.

Introduction

RTK GPS Technology has become a global utility in engineering survey activities. RTK GPS offers an efficient means of providing near instantaneous positions by employing differential GPS positioning whereby users can obtain centimetre/sub-centimetre level position in real time. In RTK GPS all algorithms using code information only are limited to range accuracy of about 0.5-1.0 metres due to code noise. However, range measurement using carrier phase information on the other hand is limited to only 0.5-3.0 millimetre by noise. Thus the use of carrier phase measurements in high precision positioning has become indispensable. Yet in order to use the carrier phase measurements in an urban canyon environment, the user has a couple of positioning errors to deal with.

Researchers have focused on defining the different positioning error sources, studying their effects, and searching for methods to decrease, or possibly eliminate these errors in order to achieve better positioning accuracies in RTK set up in an urban canyon environment

One of the major problems is the Multipath error which occurs when GPS signals are reflected from nearby objects before reaching the antenna. Also, electrical interference occurs when secondary sources or other transmitters and receivers distort the reception of the GPS signals or affect the receiver's circuitry. These are particularly problematic for RTK GPS in an urban canyon environment, because they act as bias during the short location occupations and can prevent satellite tracking.

Another problem is the sudden jumps in the carrier phase signal from one epoch to the next. This is called cycle-slips, cycle-slips must be detected and corrected before influencing the navigation solution and before changing filter-states in the code smoothing systems.

Besides the afore-mentioned error sources with the use of carrier phase observables, other problems that are associated with RTK GPS positioning is the baseline length which tends to degrade the accuracy as the baseline length increases. This is predominantly due to atmospheric effects (ionosphere and troposphere), which become de-correlated and thus no longer cancel over longer distances through differencing algorithms.

GPS Measurement Models

The observables considered in this paper consist of double differenced between two receivers. For two receiver stations (1 and 2) tracking simultaneously the same set of satellites (*s* and *l*), we have the code double difference equation for dual frequencies as

$$\text{L1:}\quad R^{sl}_{p,12} = \rho^s_1 - \rho^l_1 - \rho^s_2 + \rho^l_2 + I^{sl}_{12} + T^{sl}_{12} + M^{sl}_{p,12} - e^{sl}_{p,12} \qquad (1)$$

$$\text{L2:}\quad R^{sl}_{q,12} = \rho^s_1 - \rho^l_1 - \rho^s_2 + \rho^l_2 + (f_1/f_2)^2 I^{sl}_{12} + T^{sl}_{12} + M^{sl}_{q,12} - e^{sl}_{q,12} \qquad (2)$$

Subscripts *p*, *q* are used to identify measurements with L1, L2 with frequency f_1 and f_2 respectively.

T^{sl}_{12} is for the tropospheric delay, I^{sl}_{12} is for the ionospheric delay, M^{sl}_{12} is for the multipath delay and e^{sl}_{12} denotes an error for code observations. Similarly, for the combined phase measurements we have

$$\phi^{sl}_{p,12} = \rho^s_1 - \rho^l_1 - \rho^s_2 + \rho^l_2 - I^{sl}_{12} + T^{sl}_{12} + \lambda_p N^{sl}_{p,12} + M^{sl}_{p,12} - \varepsilon^{sl}_{p,12} \qquad (3)$$

$$\phi^{sl}_{q,12} = \rho^s_1 - \rho^l_1 - \rho^s_2 + \rho^l_2 - (f_1/f_2)^2 I^{sl}_{12} + T^{sl}_{12} + \lambda_q N^{sl}_{q,12} + M^{sl}_{q,12} - \varepsilon^{sl}_{q,12} \qquad (4)$$

where N^{sl}_{12} denotes ambiguities between satellites *s* and *l* and receivers *1* and *2*, while λ_p, λ_q are the wavelengths of L1, L2 carrier respectively, ε^{sl}_{12} is the error in the carrier phase measurements. One should note here that the above model is equally valid for the future GPS L5 frequency as well.

The double difference code and carrier phase measurements can now be reduced to the form given in equation (5)

$$\begin{aligned}
R_1 &= \rho + I + T + M_{p1} - e_1 \\
R_2 &= \rho + (f_1/f_2)^2 I + T + M_{p2} - e_2 \\
\phi_1 &= \rho - I + T + \lambda_1 N_1 + M_{q1} - \varepsilon_1 \\
\phi_2 &= \rho - (f_1/f_2)^2 I + T + \lambda_2 N_2 + M_{q2} - \varepsilon_2
\end{aligned} \qquad (5)$$

where $f_1/f_2 = 154/120 = 1.2833333....$

Multipath

Multipath signal propagation has remained a dominant cause of error in RTK GPS positioning. Multipath errors are due to reflected GPS signals from surfaces (such as buildings, metal surfaces etc) near the receiver, resulting in one or more secondary propagation paths. These secondary-paths signals, which are superimposed on the desired direct path signal, always have a longer propagation time and can significantly distort the amplitude and phase of the direct-path signal (Iyiade and Owusu-Nkasah, 2002, Cross et al, 2003).

Multipath error is scaled according to wavelength and is generally therefore nearly 100 times lager for P-code pseudoranges than it is for carrier phase measurements. Instantaneous multipath error can be as large as a few meters for P-code and a few centimetres for carrier phase. Thus, multipath becomes a dominant source of error in the measurement, in a situation in which range and phase data are needed instantaneously.

Wavelength Resolution

In resolving for the ambiguity, the combinations of wide-lane and narrow-lane observables are mostly used. The wide-lane observable provides faster solution than using either L1 or L2 observables (Cardoza et al, 1994). The combinations are

$$\phi_w = \left(\frac{\phi_1}{\lambda_1} - \frac{\phi_2}{\lambda_2} \right) \lambda_w = \rho - \left(\lambda_2 / \lambda_1 \right) I + T + M + \lambda_w N_w - \varepsilon_w \tag{6}$$

$$\phi_N = \left(\frac{\phi_1}{\lambda_1} - \frac{\phi_2}{\lambda_2} \right) \lambda_N = \rho - \left(\lambda_2 / \lambda_1 \right) I + T + M + \lambda_N N_N - \varepsilon_N \tag{7}$$

where $N_w = N_1 - N_2$ and $N_N = N_1 + N_2$ are wide-lane and narrow-lane ambiguities respectively, and the corresponding wavelength as $\lambda_w = \lambda_1 \lambda_2 / \left(\lambda_2 - \lambda_1 \right) \cong 86.4cm$ and $\lambda_N = \lambda_1 \lambda_2 / \left(\lambda_2 + \lambda_1 \right) \cong 10.7cm$.

Extended Kalman Filtering (EFK)

The EKF describes the evolution of the states, the measurement model relates the state vector to the GPS observations through the design matrix H. Regular updates by the measurement into the state vector is crucial as the system will diverge if there is no measurement provided over a long period of time, driven by the system input noise. The observations for the float filter are double difference carrier phase and code observables.

The advantage of using a filter here is that with more measurements available, the estimation of the float solution is more accurate and also reduces the size of the search space.

In summary, the process and measurement models for the extended Kalman Filter are given by

$$x_k = F(\hat{x}, k-1) x_{k-1} + w_{k-1} \tag{8}$$

$$z_k = H(\hat{x}, k) x_k + v_k \tag{9}$$

The symbol w_k and v_k denotes variance of the process noise and are zero-mean normal distributed white noise and characterized by covariance matrices Q and R respectively. The essential implementations for the extended Kalman filter are given as:

$$\hat{x}_k^- = f(\hat{x}_{k-1}^+, k-1) \quad (10)$$

$$P_k^- = F_{k-1}P_{k-1}^+ F_{k-1}{}^T + Q_{k-1} \quad (11)$$

$$K_k = P_k^- H_k{}^T \left[H_k P_k^+ H_k{}^T + R_k\right]^{-1} \quad (12)$$

$$P_k = \left[I - K_k H_k\right]P_k^-$$

$$\hat{x}_k^+ = \hat{x}_k^- + K_k(z_k - \hat{z}_k) \quad (13)$$

where $H_K \approx \left.\frac{\partial h(x,k)}{\partial x}\right|_{x=\hat{x}_k^-}$

In the static model, the state transition matrix F_k can be described as

$$F_k = \begin{bmatrix} 1 & 0 & 0 \\ 0 & 1 & 0 \\ 0 & 0 & 1 \end{bmatrix} \quad (14)$$

For static positioning, the state vector contains only the position, and w_k is set to a small number. The measurement equation can be written as in equation (9)

$$H_k(x_k) = \left[R^1, R^2, R^3, R^4\right]_K^T \quad (15)$$

R^1, R^2, R^3, R^4, are the measurement consists of pseudorange and phase observation and hence the relation between the measurements and the states (position vector) is not linear. Equation (15) can be linearised by approximating $H_k(x_k)$ with Taylor series expansion about the predicted value of the states $\hat{x}_k^-$ at $t = k\Delta t$ and retaining only the first-order terms (equation 17). The linearised measurement equation in the extended Kalman filter is defined as

$$z_k = Hx_k \quad (16)$$

where H is the Jacobian matrix given as follows

$$H = \begin{bmatrix} u_1^1 - u_2^k \\ u_1^2 - u_2^k \\ \dots \\ u_1^n - u_2^k \end{bmatrix} \quad (17)$$

where

$$u_1^k = \frac{x_{ECEF}^K - x_1}{\rho_1^k}, \frac{y_{ECEF}^K - y_1}{\rho_1^k}, \frac{z_{ECEF}^K - z_1}{\rho_1^k} \qquad (18)$$

The measurement vector *z* is expressed as

$$z = \begin{bmatrix} \phi_{q,12}^{k1} - \lambda_q N_{q,12}^{k1} \\ \phi_{q,12}^{k2} - \lambda_q N_{q,12}^{k2} \\ \dots \\ \phi_{q,12}^{kn} - \lambda_q N_{q,12}^{kn} \end{bmatrix} \qquad (19)$$

In the dynamics model of the filter, three states which will be nine variables that are three linear degrees of freedom (position vector), the correspondence velocity variables (velocity vector) and correspondence acceleration variables (acceleration vector) are considered. In this application, the state model can be written as

$$X_k = [x, v_x, a_x, y, v_y, a_y, z, v_z, a_z]_k^T \qquad (20)$$

This model can be represented by the equation

$$\begin{aligned} x_{k+1} &= x_k + \Delta t v_x + \frac{\Delta t^2}{2} a_x \\ y_{k+1} &= y_k + \Delta t v_y + \frac{\Delta t^2}{2} a_y \\ z_{k+1} &= z_k + \Delta t v_z + \frac{\Delta t^2}{2} a_z \end{aligned} \qquad (21)$$

The relation between the previous states and the current states are govern by the transition matrix (F_k),

$$F = \begin{bmatrix} 1 & 0 & 0 & \Delta t & 0 & 0 & \Delta t^2/2 & 0 & 0 \\ 0 & 1 & 0 & 0 & \Delta t & 0 & 0 & \Delta t^2/2 & 0 \\ 0 & 0 & 1 & 0 & 0 & \Delta t & 0 & 0 & \Delta t^2/2 \\ 0 & 0 & 0 & 1 & 0 & 0 & \Delta t & 0 & 0 \\ 0 & 0 & 0 & 0 & 1 & 0 & 0 & \Delta t & 0 \\ 0 & 0 & 0 & 0 & 0 & 1 & 0 & 0 & \Delta t \\ 0 & 0 & 0 & 0 & 0 & 0 & 1 & 0 & 0 \\ 0 & 0 & 0 & 0 & 0 & 0 & 0 & 1 & 0 \\ 0 & 0 & 0 & 0 & 0 & 0 & 0 & 0 & 1 \end{bmatrix} \qquad (22)$$

where Δt is the time step between t_{k-1} and t_k (transition time interval in seconds), and the process noise vector w_k is considered to be zero mean white.

The *H* matrix is the same as that of the static section only that it is expanded with zeros considering the velocity and the acceleration vectors. Hence the *H* matrix in the kinematic state now becomes a 2*n*x9 matrix. Observation vector is however the same as the static model. In implementing the EKF the initial estimates of the state vector, the corresponding velocity and acceleration components were obtained from the first epoch measurement. In the EKF models the parameters used in initializing the filters are the same. However, there are differences in the size of the matrices which change to reflect the state estimates.

It is important to note here that the covariance matrix is actually an estimate of the statistics of the estimation error vector. Wrongly modelling of the system dynamics or of the process or measurement noises can cause the true estimation error uncertainties to be quite different from the covariance matrix computed by the filter. Modelling only a subset of the total set of errors (suboptimal filter) will also cause an inaccurate covariance matrix. When this occurs, the accuracy of the positioning may be substantially degraded. The process whereby the covariance matrix of the mechanized filter is made to closely approximate the true covariance matrix is referred to as Kalman filter tuning.

One way in which GPS Kalman filters are often tuned is through the use of adaptive tuning. Specifically, this refers to dynamically setting the process noise Q as a function of vehicle motion. This approach is used in accounting for wrong modelling in the state dynamics model. In this case, the errors are not Gaussian noise, but may be biases in turns. Therefore, the correct Q depends on the vehicle profile.

Signal to Noise Ratio (SNR)

The power of a GPS signal is the basic measure of its quality. The power levels of GPS signals are usually specified in terms of decibels with respect to 1 watt of power (dBw). The minimum received power levels of the GPS signals for the users on Earth are {160 dBw and {166 dBw for L1 and L2, respectively (NAVSTAR GPS, 1995). The most common signal quality measures that can be used for weighting are the signal-to-noise ratio (SNR) and the carrier-to-noise power density ratio (C/N_0).

The SNR is the ratio of the amplitude of the desired signal to the amplitude of noise signals at a given point in time. The SNR is generally used as a measure of the noise level that can contaminate a GPS observation. This value can be compared with the power of a GPS signal. The ratio of the power of a received signal, *S*, and the noise power, *Ns*, can be considered a measure of strength.

A high SNR value is highly desirable. The C/N_0 in GPS receivers is the ratio of the power level of the signal carrier to that of the noise in a 1 Hz bandwidth. Nominal GPS receiver C/N_0 values often are in the 30 to 60-dB-Hz range. The C/N_0 describes the ratio of the power level of the signal carrier to the noise level in an influence on the C/N_0 value. It is a key parameter in analyzing GPS receiver performance and directly affects the precision of the receiver's pseudorange and carrier phase observations.

Quality Control

In handling various alternative hypothesis, the Detection, Identification and Adaptation (DIA) method as described by (Teunissen, 1998) was implemented in the software used in processing the observed data. The DIA-procedure consists of the followings steps (de Jong, 1998):

- Detection: In the detection step, a global overall model test is performed on the whole observation set at a given epoch in other to check weather unspecified model errors have occurred.
- Identification: After detecting of model errors, identification of the potential source of these errors is required. After identification, the detected bias is compared with the Minimal Detectable Biases (MDB) value that is a

threshold value used to identify biases. If the bias candidate's value is less than the MDB value, the observation is accepted.

- Adaptation: After identification of the alternative hypothesis, adaptation of the recursive filter is needed to eliminate the presence of biases in the state estimation.

How well observations are controlled is a function of the redundancy in the observations. Redundancy numbers could be defined as elements of the principal diagonal of matrix $(P_{\hat{r}}P_l^{-1})$. The redundancy of the ith observation can be expressed as

$$Rd_i = \left(P_{\hat{r}}P_l^{-1}\right)_{ii} \tag{23}$$

where the subscripts ii indicates the ith diagonal element of the matrix and $P_{\hat{r}}$ is the covariance of the residual. The trace of *Rd* is the observation redundancy (υ), since *Rd* is idempotent (unchanged in value following multiplication by itself) and the trace of an idempotent matrix equals its rank (Leick, 1995). Each diagonal element of *Rd* corresponds to that observation's contribution to the overall redundancy. Assuming that the observation is uncorrelated (that is the observation covariance matrix is diagonal), the diagonal elements (ν_i) is

$$\nu_i = \frac{P_{\hat{r}_{ii}}}{P_{l_{ii}}} \tag{24}$$

The MDB is the smallest error on a particular observation which the model or system will be able to detect. The MDB for the ith observation can be expressed as (Lachapelle and Ryan, 2000)

$$\left|\nabla_i\right| = \frac{\delta_0}{\sqrt{Rd_i}}\sigma_{l_i} \tag{25}$$

where σ_{l_i} is the standard deviation of the *ith* observation and $\left|\nabla_i\right|$ is the magnitude of the N by 1 vector ∇_i.

Experiments

The elevation angle information is often used in the construction of the stochastic model. The reason for using the satellite elevation angle is because each satellite has a different precision and it is known that low elevation angle satellite tends to be noisier than the higher elevation angle satellite.

Figure 1: Shows elevation angles, C/N_0 and number of satellites tracked during the experimental period. During the observation period, some satellites dropped out of view while some were reacquired shortly after an example of this is PRN 2 and PRN 15. The increase in C/N_0 variations for descending and rising satellites illustrates the increase multipath on these signals at lower elevation angles.

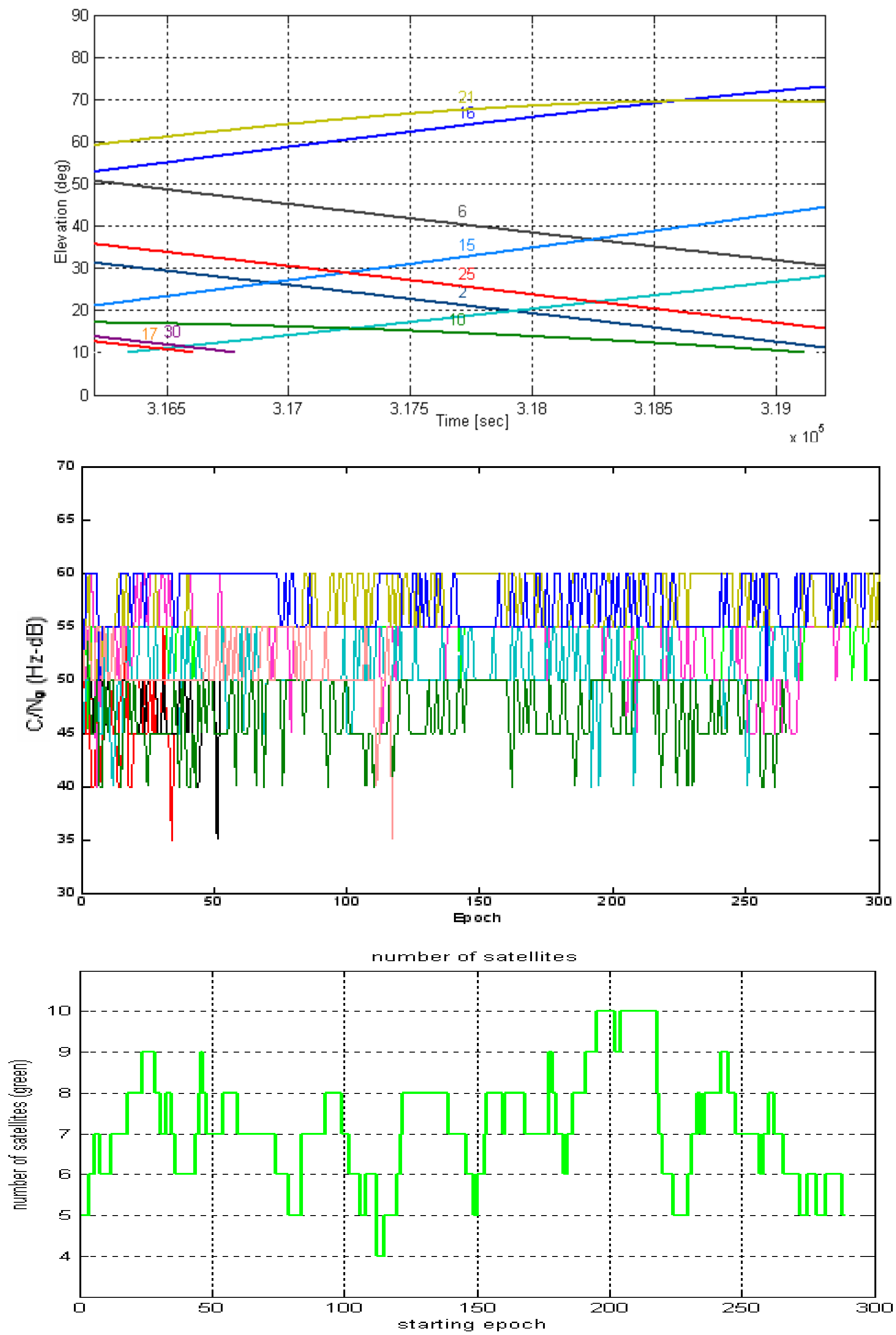

Figure 1: Depicts Elevation angles, C/N_0 and the number of satellites tracked during the observation period. Some satellites orbited out of view while new ones were tracked. The minimum number of satellites tracked was four, and the maximum tracked was 10.

During the observation period PRN 17 and PRN 30 orbited out of view, while there was constant loss of lock with PRN 15 during this period. Figure 2 depicts the multipath error of the satellites tracked on L1.

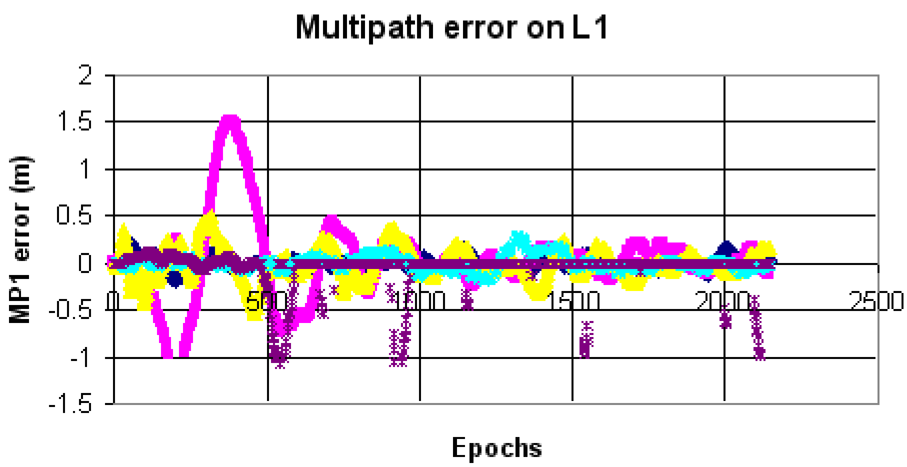

Figure2 shows the multipath error on L1 for all the tracked satellites, from the plot it could be seen that there were loss of lock in some of the satellites during the observation period. The most affected PRN is 15 which happened frequently.

Figure 3, shows the estimation of the multipath parameters with the implementation of an extended Kalman filter, the initial results were not too bad. In the EKF process, each new estimate is re-linearised as it becomes available, hence the filter worked well as it is near their true values.

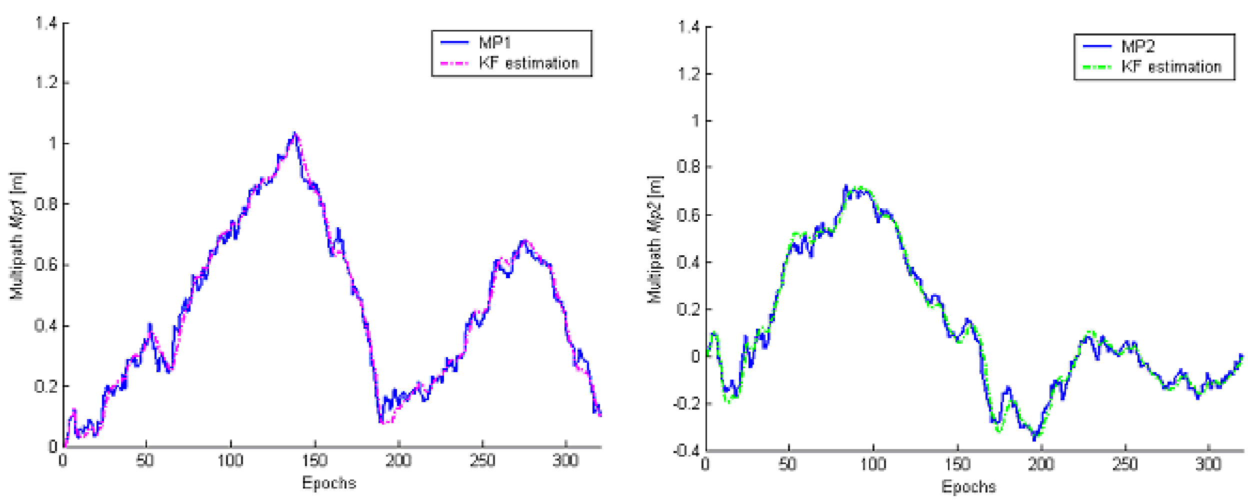

Figure 3: Double difference multipath error on L1 (left) and L2 (right). The filtered multipath errors are in dotted lines. Only a portion of the observation is shown here. The filtered value did not deviate too much from their true values.

Figure 4 shows the north, east and the height position errors over time, The GPS error becomes noisy and it is expected that the error should drop with increasing satellite number, however the overall results show an improved position coordinates.

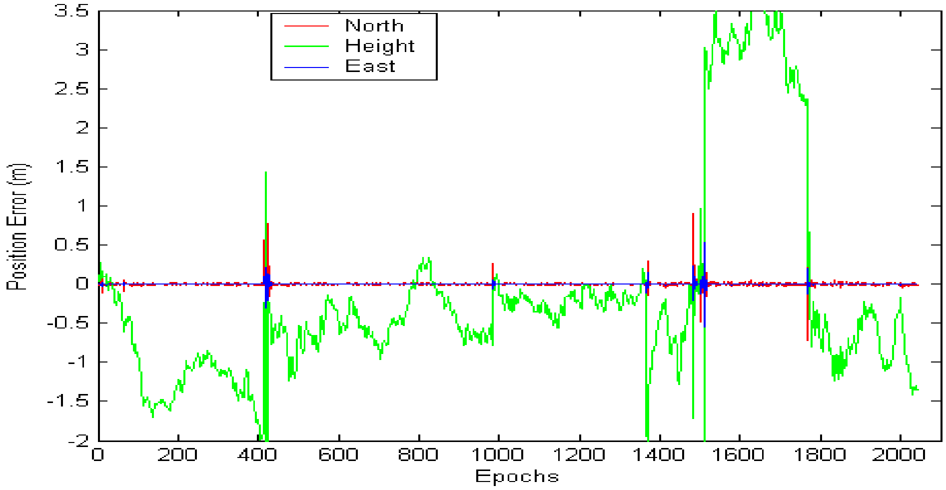

Figure 4: Positioning error showing the north (red), east (blue) and height (green) components. The data recording for this test was at the rate of 1 sample every 10seconds. The height components showed some strange characteristics, this is due to the measurement noise. The fact that multipath of such magnitude might be present in the carrier phase measurements limits the accuracy of the positioning. More so, it is known that multipath shows periodic behaviour, the periods can be in the order of minutes and also depends on the reflecting object.

Conclusion

The limiting factors in attaining better accuracy in GPS observations in the urban canyon environment is the multipath. Multipath errors increase when the line of sight approaches the horizon that is the higher the satellite elevation angle the lower the carrier phase noise. More so other GPS errors can be eliminated by data differencing in time domain as long as the observation time are time-correlated. The use of Kalman filtering reduced the noise in other to achieve a better positioning accuracy. Finally, statistical testing can be efficient if the stochastic models are correctly known or well estimated. There are rooms for improvement in this paper, so a lot of research works still need to be done.

Reference:

[1] Barnes J.B, Ackroyd N, Cross P.A. Stochastic Modelling For very High Precision Real-Time Kinematics GPS in An Engineering Environment. XXI Congress of the International Federation of surveyors (FIG), Prat 6, Paper TS13, pp61-76, 1998.

[2] Brown N, Williamson I, Kealy A. Stochastic modelling of GPS Phase Observations. FIG XXII International Congress, Washington D.C, April 19-26, 2002.

[3] Brown R.G (1983) Introduction to Random Signals and Kalman Filter. John Wiley and Sons, pp 296-297.

[4] Cardoza M.A, Leah M.P, Tucker A.C. Field Results from a Realtime Precise Positioning System. Institute of Navigation. 1994.

[5] Cross P, Betaille D, Peyret F. Improving GPS Accuracy for Construction Applications through Phase Multipath Mitigation. Proceedings of GNSS 2003, Tokyo, Japan. pp 123 – 132.

[6] de Jong C.D. Genration of DGPS/DGlonass corrections including quality control. Proceedings INSMAP98, Melbourne, FL, USA, November 30 - December 4, 1998.

[7] Gelb A. (1974), Applied Optimal estimation. MIT press Cambridge Massachusetts.

[8] Hofmann-Wellenhof B, Lichtengger H and Collins J, (2001). GPS Theory and Practice, Fifth Edition. Springer Wien, New-York. Pp 97-115; 124-131; 138-139; 205-206; 213-244; 252-255.

[9] Iyiade A and Owusu-Nkasah K. Real-time Kinematic GPS. Institute of Electronics Systems (IES), Aalborg University. Denmark. 2002.

[10] Jin X and Lu S, The MPP program (version 7.0) Unpublished.

[11] Kim D and Langley R.B. Quality Control Technique and Issues in GPS Applications: Stochastic Modelling and Reality Test. International symposium on GPS/GNSS (the 8th GNSS workshop), Jeju Island South Korea. November 7- 9, 2001.

[12] Lachapelle G and Ryan S. Statistical Reliability Measure for GPS. IMA Workshop on Mathematical Challenges in GPS, August 16-18, 2000.

[13] Leick A, (1995). GPS Satellite Surveying. John Wiley and Sons, second edition, pp 108-109; 247-262; 301-316; 352-356; 388-391.

[14] NAVSTAR GPS, Global Positioning System Standard Positioning Service Signal Specification, Second Edition, June 2nd, 1995

[15] Strang G and Borre K, (1997). Linear Algebra, Geodesy, and GPS. Wellesley-Cambridge Press. Pp 455-456; 459; 460-465; 509-511; 523-527

[16] Teunissen P.J.G, de Jonge P.J, Tiberius C.C.J.M (1995) The LAMBDA-Method for fast GPS Surveying. Presented at the International Symposium "GPS Technology Applications" Bucharest, Romania, September 26-29, 1995.